Developmental regulation and evolution of cAMP signalling in Dictyostelium

Alvarez-Curto, E.

Chapter Four

Molecular phylogeny and evolution of morphology in the social amoebas

Abstract

The social amoebas (Dictyostelia) display conditional multicellularity in a broad variety of forms. Apart from the genome sequence of *Dictyostelium discoideum*, there is little molecular data from the rest of the group. This Chapter introduces the first dictyostelid molecular phylogeny using two parallel datasets - small subunit ribosomal RNA and α-tubulin. The phylogeny shows a molecular depth for Dictyostelia similar to animals, and indicates that their taxonomy requires complete revision. A mapping of well-documented characters onto the phylogeny identifies increased size and cell-type specialization of fruiting structures, but not architectural complexity, as trends in dictyostelid evolution. This major taxon is now uniquely well suited to identify molecular changes underlying phenotypic innovation.

Introduction

Animals and plants display an enormous variety of forms, but their underlying genetic diversity is relatively small compared to the immense genetic diversity of the microbial world. Eukaryotic microbes include a broad range of morphologically or physiologically distinct unicellular life forms, with multiple independent and novel inventions of multicellularity. One of the most intriguing and challenging problems in biology is to understand how the latter has happened, and why this particular evolutionary stratagem has repeatedly arisen.

The social amoebas or Dictyostelia (*1*) are a striking group of organisms that hover on the borderline between uni- and multicellularity. Their life cycle consists of a unicellular feeding stage that can take three directions when cells are starved. i) Individual cells may encyst to form microcysts (*2*). ii) Cells fuse and two nuclei combine to form a zygote that subsequently cannibalizes neighboring cells and then encapsulates to form a macrocyst. iii) Numerous cells may aggregate and differentiate to form a multicellular fruiting body consisting of spore and stalk cells. Microcysts represent the ancient survival strategy of the solitary amoebas from which the social amoebas arose (*3*). Apart from the cannibalistic attribute of the dictyostelid macrocyst, zygotic cyst formation is also a common survival strategy for a diversity of eukaryotes from green algae to dinoflagellates to fungi.

Thus, it is the process of fruiting body formation in social amoebas that has long fascinated developmental biologists. This has been best described for the model organism *Dictyostelium discoideum*. Here the aggregate of up to 100,000 cells first encases itself in a skin-like matrix, and then transforms into a macroscopic finger-shaped structure, the "slug". This slug possesses specialized head and body regions whose roles in the final fruiting structure are now set. The head region senses environmental stimuli such as temperature and light, and directs migration of the slug towards the soil's outer surface, where spores will be most readily dispersed. Migration ends with the slug "standing up" to form the fruiting body or sorocarp. The cells in the head region first deposit a cellulosic stalk tube; they then move into this tube, swell up, deposit more cellulose and die. The remaining "body" cells then crawl up this newly formed stalk and encapsulate to form spores. Thus the Dictyostelia display distinct characteristics of true multicellularity, such as cell-cell signalling, cellular specialization, body axes formation, coherent cell movement and altruism.

Traditionally, classification of the social amoebas has been based on their most striking trait, fruiting body morphology. Based on this, three genera were proposed: *Dictyostelium*, with unbranched or laterally branched fruiting bodies, *Polysphondylium,* whose fruiting bodies consist of repetitive whorls of regularly spaced side branches, and *Acytostelium*, which, unlike the other genera, forms acellular fruiting body stalks (*2*).

Despite the widespread use of *D. discoideum* as a model organism (*4,5*), the Dictyostelia as a whole are very poorly characterized in molecular terms, with nearly all currently available data being from a single species. Nonetheless, the social amoebas provide us with a unique opportunity to understand the evolution of multicellularity (*6-8*). A primary and essential prerequisite for this is an accurate and complete understanding of the true phylogeny of the group. Only then can we meaningfully correlate the history of phenotypic change with the history of genetic change and begin to infer the molecular genetic modifications that led to the

generation and diversification of multicellular life. This work describes the first reconstruction of the tree of life of most known social amoeba species, and traces the acquisition of morphological and functional complexity during their evolution.

Material, methods and supporting material

Cell culture and genomic DNA extraction

All species were cultured on LP agar (1). When necessary, fruiting body formation of the more delicate species was facilitated by placing about 20 pellets of activated charcoal in the petri dish lid. To isolate genomic DNA, cells were harvested and washed three times with 10 mM K-phosphate buffer pH 6.5. Around 3×10^7 cells were lysed in 1 ml HMN (10 mM NaCl, 30 mM Mg-acetate, 10% (w/v) sucrose and 0.5% (v/v) Nonidet P-40 in 30 mM HEPES, pH 7.5), and nuclei were pelleted by centrifugation for 5 minutes at 6500 rpm. Pellets were resuspended in 50 µl HMN and 150 µl of resuspension solution from the GenElute Mammalian Genomic DNA Kit (Sigma, St.Louis, USA). Further DNA isolation was performed according to the kit's protocol.

PCR amplification, cloning and DNA sequencing

PCR and sequencing of SSU rDNA. A ~2000 base pair (bp) fragment of SSU rDNA was amplified by PCR (2) using primers A (forward) and B (reverse) as previously described (*3*) with 50°C annealing. Following amplification, PCR products were separated on 1% agarose gels, and appropriate sized bands excised and extracted from the gel, using the QIAquick gel extraction kit (Qiagen, Crawley, UK). Purified DNA was then cloned into the pGEM-T easy T-tailed vector (Promega, Southampton, UK) and transformed into DH5α competent cells (Invitrogen, Paisley, UK). A minimum of eight positive colonies were screened by PCR using flanking primer sequences (Sp6 and T7) to confirm the presence of inserts and to screen for possible multiple products (4). For sequencing, DNA was first amplified by PCR using the T7 and SP6 primers, precipitated with polyethylene glycol and processed further as described (3). Two clones for each PCR product were sequenced completely on complementary strands using the T7 or SP6 primers and one walking primer (forward primer D542-F: 5'-ACAATTG-GAGGGCAAGTCTG-3'; reverse primer D1340R: 5'-TCGAGGTCTCGTCCGTTATC-3'). To control for a possible multiple of SSU rRNA genes in *P. violaceum*, 50-150 PCR product clones for each of three independent isolates were screened by restriction fragment polymorphism (RFLP) analysis (3). Sequencing was performed using ABI PRISM BigDye Terminator v3.0 (Applied Biosystems) on a 3730 DNA Analyzer at the Oxford Sequencing Facility (http://polaris.bioch.ox.ac.uk/dnaseq/). Sequences were initially analyzed using Chromas version 2.23 (Technelysium Pty ltd) and then assembled into contigs using BioEdit version 5.0.9 (5).

PCR and sequencing of α-tubulin (tubA). Amplification, cloning and sequencing of *tubA* followed the same protocol as above except for using the primers atF3 and atR3 (*3*). Some *tubA* PCR reactions also required annealing at 40°C, and others required a second round of amplification using 1µl of the original reaction as substrate in order to obtain sufficient material for cloning. A minimum of 12 positive clones from each PCR product was screened by reamplification and size fractionation, which always yielded only identical sized clones from any given DNA. Two clones were then sequenced completely on complementary strands. Since *tubA* reactions utilized degenerate PCR primers, some reactions yielded multiple products of the correct or larger size. In all cases, these additional products were also cloned, screened and completely sequenced. However, in no case were multiple *tubA* genes detected.

Multiple sequence alignment

Alignment of SSU rDNA sequences consisted of five steps. 1) Based on a rough preliminary phylogeny, sequences were assigned to one of four major groups. 2) Sequences for

each group and for the amoebozoan outgroup were each aligned separately in ClustalX (*6*) using default parameters. 3) Each alignment was imported separately into the alignment editor Bioedit (*5*) where minor modifications were made by eye to minimize hypothetical insertion-deletion events, and 70% consensus sequences were calculated (also 50% and 60% sequences for amoebas). 4) The resulting consensus sequences were imported into PAUP* (*7*) and aligned to each other by eye along with individual sequences not obviously belonging to any group (*D. polycarpum, D. polycephalum, P. violaceum, D. laterosorum*). 5) Finally, the five separate alignments were imported into the same file. These were aligned to each other following their respective consensus sequences in the master consensus alignment, with minor final adjustments made by eye.

Only unambiguously aligned regions of the SSU rDNA alignment were used for phylogenetic analyses. These were defined as regions bordered by a consensus sequence entry for all Groups and with no internal insertions or deletions greater than 1 nucleotide in length (1674 sites). In order to resolve the highly similar Group 4 sequences, separate analyses were conducted including additional sites only alignable within the group (1861 total sites). The position of the Dictyostelia root was tested using only sites alignable among all 4 groups plus the amoebas (1374 sites). Very little length variation is seen in α-tubulin across all eukaryotes (*8*). Therefore, tubA nucleotide sequences were aligned manually in Bioedit (*5*) and then automatically translated into amino acids following intron removal. All analyses were conducted at the amino acid level, and all sites were included.

Phylogenetic analysis

Bayesian inference. Bayesian inference was used to calculate posterior probability of clades (biPP) utilizing the program MrBayes (version 3.1 or 3.1.1) (*9*). Final analyses consisted of two sets of four chains each (one cold and three heated) run for 1-10 million generations with trees saved every 10 generations and parameters sampled every 100. All analyses were run at least until a split frequency of <0.01 between the two run sets was reached. Posterior probabilities were averaged over the final 75% of trees (25% burn in), which was well passed convergence (log probability plateau, usually reached within <10,000 generations) for all analyses. Bayesian analyses of SSU rRNA sequences utilized the general time reversible model with a proportion of sites designated invariant, and rate variation among sites modelled after a gamma distribution divided into six categories (GTR+I+G) (*10*), with all variable parameters estimated by the program based on BioNJ starting trees. Amino acid sequences of α-tubulin were analyzed using a mixed amino acid model with sites again weighted according to a six-category gamma distribution and relevant parameters estimated by the program as above.

Maximum likelihood. Maximum likelihood was used to calculate bootstrap support values (mlBP) utilizing the program PHYML (*11*) over the web (http://atgc.lirmm.fr/phyml /) or on a PC. A total of 500 (web-based analyses) or 1000-10,000 bootstrap replicates were conducted using the GTR+I+G model for SSU rRNA and the WAG+I+G model (*12*) for amino acids. All variable parameters were estimated using the program from BioNJ starting trees.

Phylogenetic controls. All sets of analyses were also conducted with sequential and combined exclusion of relevant disproportionately long-branched sequences (overall tree and root analyses – *D. multistipes, A. ellipticum, D. polycarpum, Planoprotostelium, Thecamoeba*; Group 4 analyses - *D. septentrionalis*). From these results it was determined that neither topology nor support values were substantially affected by long-branches (*13*). That is, there were no changes in the significantly resolved portions of the topology (clades with mlBP>70% and/or biPP>0.90), and no substantial change in support values (mlBP +/- 5%, biPP +/- 0.01).

Combined sequence analyses. Combined analyses utilized concatenated alignments of SSU rRNA with either α-tubulin deduced amino acid sequences (tubA-AA) or first and second codon position nucleotides (tubA-NT). Differential weighting of the α-tubulin matrix was also performed in an attempt to compensate for the roughly 2 or 4 fold difference in the number of phylogenetically informative sites between SSU rRNA versus tubA-NT and tubA-AA datasets (564, 273 and 161 parsimony informative sites, respectively). Weighting was

accomplished by double, triple or quadruple entry of the tubA (NT or AA) matrix. Bayesian analyses utilized separate models for each data type (partition), with separate GTR+I+G models for SSU rRNA and tubA-NT, and a mixed amino acid model tubA-AA.

Maximum likelihood (PHYML) and paralinear distance (LogDet) analyses were performed at the nucleotide level only (SSU rRNA + tubA-NT), as mixed nucleotide and amino acid model implementations are not currently available for either of these methods. PHYML analyses were performed as described above. LogDet analyses were performed under the minimum evolution model with PAUP 4b10 (7) and a fraction of 0.34 sites designated as invariant as estimated by the program based on an initial neighborjoining tree calculated under the Kimura 2-parameter model (14). Analyses consisted of 1000 bootstrap replicates with trees derived by neighborjoining.

Results

Molecular phylogeny of Dictyostelia

Nearly complete small subunit ribosomal RNA (SSU rRNA) gene sequences were determined from over 100 isolates of Dictyostelia, including nearly every described species currently in culture worldwide. Phylogenetic analyses of these data identify four major sub-divisions of the group, here numbered 1 to 4 (Fig. 1). Group 1 consists of a morphologically diverse set of *Dictyostelium* species. Group 2 is a mixture of species with representatives of all three traditional genera including all pale coloured species of *Polysphondylium*, at least two species of *Dictyostelium*, and all species of *Acytostelium*. Group 3 is again a diverse set of purely *Dictyostelium* species, also including the single cannibalistic species, *D. caveatum*. The largest group is Group 4, which consists almost entirely of *Dictyostelium* species possibly also including a clade of two violet colored species from two separate traditional genera, *P. violaceum* and *D. laterosorum*. With the exception of the latter, Group 4 is a fairly homogeneous set of large robust species including the model organism *D. discoideum* and the cosmopolitan species, *D. mucoroides*, which appears to be polyphyletic (9t).

These four SSU rRNA (rDNA) groupings are confirmed by α-tubulin phylogeny (Fig. 2) with two exceptions: i) *A. ellipticum* is only weakly placed with Group 2 in the α-tubulin tree (Fig. 2), and in fact appears as a poorly supported independent branch with maximum likelihood (not shown, 27t). ii) The *D. laterosorum* plus *P. violaceum* clade is grouped together with *D. polycephalum* as the sister group to a weakly supported Group 3 plus 4 clade (0.64 Bayesian inference posterior probability (biPP), 51% Maximum likelihood bootstrap (mlBP)), rather than as the exclusive sister lineage to Group 4 as in the SSU rRNA tree (Fig. 1). Weak resolution of the *A. ellipticum* branch and several other deep branches in the α-tubulin tree may be due to the much smaller size of this molecule versus SSU rRNA (322 and 1655 variable sites, respectively). Resolution of the position of the *D. laterosorum* plus *P. violaceum* clade may be further complicated by the accelerated evolution of α-tubulin sequences in Group 4 (Fig. 2) (*10*).

One taxon in particular, *D. polycarpum*, appears as a strongly supported solo branch in the SSU rRNA tree (Fig. 1) and the combined SSU rRNA plus α-tubulin nucleotide trees (not shown). This suggests that this delicate species with bunched fruiting bodies may represent an ancient dictyostelid lineage. This would also suggest that this species may, in fact, be a collection of morphologically similar cryptic species as suggested by the considerable difference in SSU rRNA sequence between the two separate isolates of *D. polycarpum* examined (Fig. 1). This could also be the case for *D. polycephalum*, as mentioned above, another delicate species with bunched fruiting bodies that is not definitively placed with any group by either gene.

One of the most striking features of the dictyostelid molecular phylogeny is the split of the genus *Polysphondylium*. The violet coloured *P. violaceum* is unequivocally grouped together with *D. laterosorum*, which lie together at the base of Group 4 (Fig. 1) or Groups 3 plus 4 (Fig. 2). Meanwhile the pale coloured Polysphondylids are all found nested within Group 2 (Fig. 1 and Fig. 2). With regard to Group 2, the phylogenetic position of *A. ellipticum* is particularly

intriguing. Both the SSU rRNA and α-tubulin trees place this taxon on a separate branch from the other *Acytostelium*s (Figs. 1 and 2), as does elongation factor 1α (EF-1α) phylogeny (B. Elgie, P. Schaap and S. Baldauf, unpublished results). This placement is also unequivocally supported in all combined SSU rRNA plus α-tubulin trees (not shown, *27*). This would be very interesting if true, because it would mean that the pale *Polysphondylium*s evolved from an *Acytostelid* ancestor. Thus the polysphondylids would not only have invented a relatively complex morphology from a morphologically simple ancestor, but they would also have reinvented the cellular stalk.
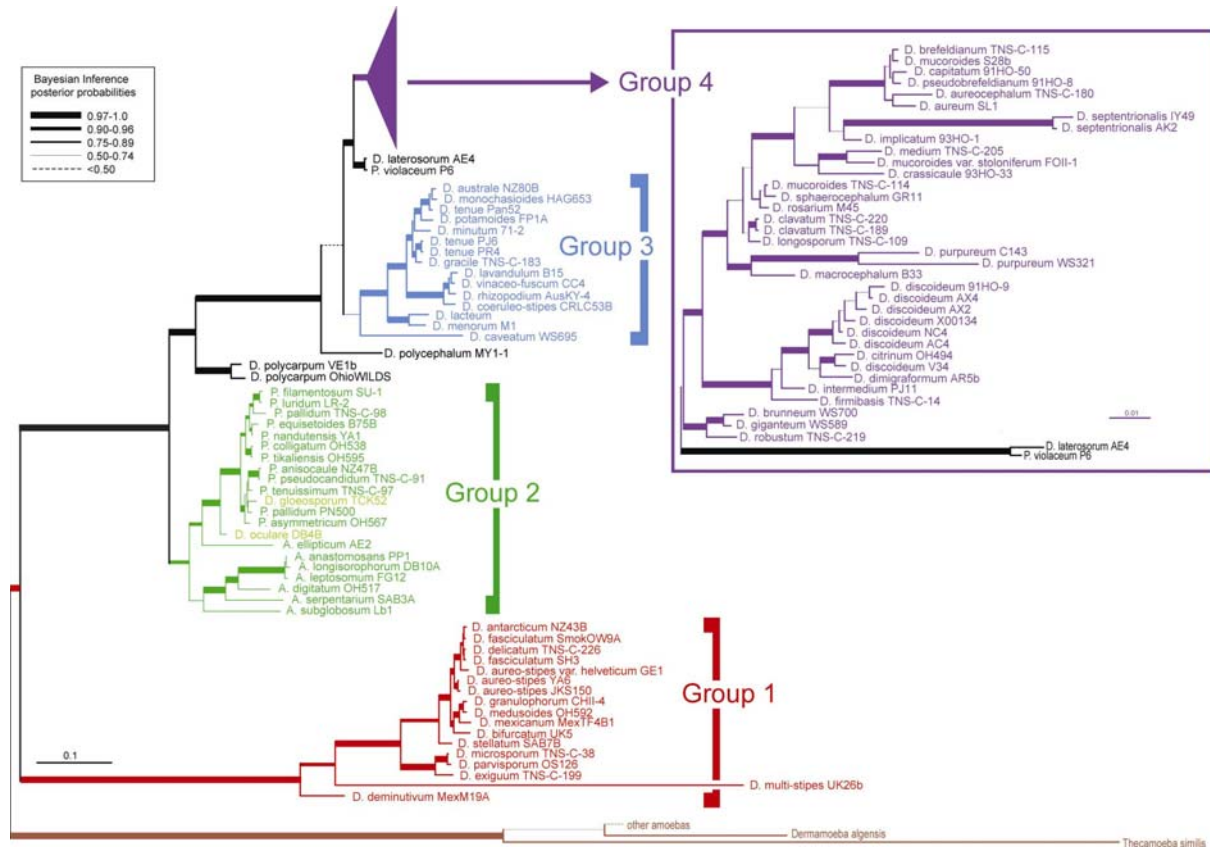

Figure 1. A universal phylogeny of the Dictyostelia based on SSU rRNA sequences
The tree shown was derived by Bayesian inference from 1655 well-aligned positions of SSU rRNA sequences. Four major taxa (Groups 1-4) are indicated by separate colours and to the right of the figure beside brackets (*Dictyostelium* species within Group 2 are indicated in lighter green). The tree includes nearly all known and described species of *Dictyostelium* (*D.*), *Polysphondylium* (*P.*) and *Acytostelium* (*A.*). Bayesian inference posterior probabilities (biPP) are roughly indicated by line width (key at the upper left of the figure). The tree is rooted based on separate analyses of 1355 positions alignable with sequences from closely related lobosan amoebas (*23, 24*). Branches lengths for the latter were scaled up to compensate for the smaller number of sites, based on the length of the first two internal branches (*27*).

The SSU rRNA phylogeny strongly supports Group 1 as the deepest major divergence in Dictyostelia (Fig. 1), as do analyses of combined SSU rRNA and α-tubulin nucleotide sequences (*27*). Although this root is not recovered in the α-tubulin amino acid phylogeny, which tentatively places Group 2 as the first major split (Fig. 2). These data only weakly resolve most of the deep branches in the tree (Fig. 2). Identifying the root of a tree is one of the most difficult problems in phylogenetic reconstruction, due to the antiquity of these events and the often-large divergences involved (*11*). Therefore, the position of the root of the dictyostelid tree still requires confirmation by broad sampling of additional genes and, eventually, combined multi-sequence analyses (*12,13*).

Initial inspection of the first taxonomically comprehensive molecular data set from Dictyostelia (Fig. 1 and Fig. 2) indicates that, at least in molecular terms, Dictyostelia is a very

deep and complex taxon. In fact, the dictyostelid SSU rRNA tree possesses a molecular depth roughly equivalent to that of a broad sampling of animals and substantially larger than that of a broad sampling of fungi.
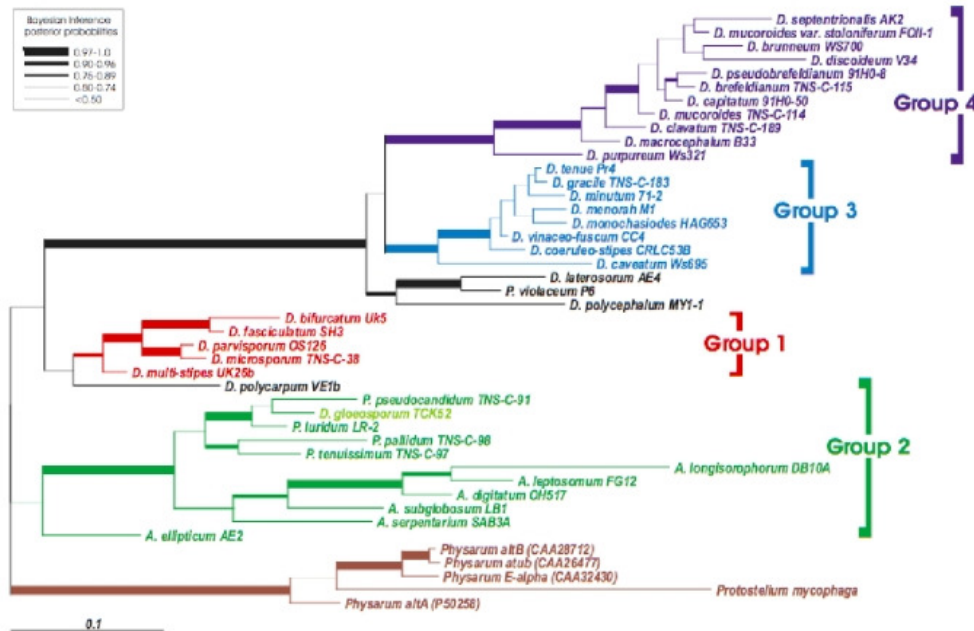

Figure 2. Phylogeny of the Dictyostelia based on α-tubulin amino acid sequences
The tree shown was derived from 322 universally aligned α-tubulin amino acid positions using Bayesian inference with a mixture of amino acid models and a six-category gamma correction. The tree includes a broad representation of all four major groups identified in the comprehensive SSU rRNA phylogeny. Colours and brackets indicate major groups with labels as in Figure 1. All biPP values are roughly indicated by line width according to the key shown in the upper left. Branch lengths are drawn to scale as indicated by the scale bar at the lower left (27).

Evolution of morphology in the Dictyostelia

Social amoeba species show striking differences in the size and branching patterns of their fruiting bodies and the presence/absence and shape of support structures. They may also vary in spore characteristics, cell aggregation patterns, slug migration characteristics and presence/absence of alternative life cycles, such as the microcyst and macrocyst. To understand how these traits might have evolved, we mapped all well-documented dictyostelid traits onto the molecular phylogeny, summarising a >50 year literature (Fig. 3). Some of the most significant traits are summarized below.

Spores and cysts. Few of the traditionally noted morphological characters show any clear trend across the tree, although a number show interesting within group trends (Fig. 3). The most globally consistent character appears to be spore shape (Fig. 3, column 2). Spores can be either round (globose) or oblong, in the latter case often with granules at their poles. Groups 1 and 3 are characterised by having oblong spores with tightly grouped (consolidated) granules. In Group 2, the granules have become loosely grouped (unconsolidated), while polar granules are lost entirely in Group 4. Group 1 is further characterised by having markedly smaller spores than the other taxa (Fig. 3, column 1).

Species that form sexual macrocysts are present in all four groups (Fig. 3, column 4). Although homothallic macrocysts are not uncommon, many species require cells of opposite mating type for sex (2). The number of species that show sexual activity is therefore probably underestimated, because the proper mates were never brought together in the laboratory.

Many species in Groups 1, 2, and 3 individually encapsulate to form microcysts, but these have not been observed for Group 4 species (Fig. 3, column 3). The number of microcyst forming spe-cies is probably also underestimated, since not every species may have been subjected to conditions that trigger this alternative survival strategy.

Aggregation and slug migration. To aggregate, cells can either come together as individuals, creating mound-shaped aggregates, or line up with each other to form inflowing streams. Stream formation is the most common mode of aggregation, with only a few species in Groups 1 and 3 aggregating as individuals (Fig. 3, column 6). The chemoattractant (acrasin) that is used for aggregation has been identified for only a few species (Fig. 3 column 5). For all investigated Group 4 species, including *D. discoideum*, the acrasin is cAMP. In Group 3, the acrasin has been identified for only three species, all of which differ: *D. minutum* uses folic acid, *D. lacteum* a pterin analog and *D. caveatum* the modified dipeptide glorin (Fig. 3, column 5). The latter may be fairly widespread, since it is used as acrasin in Groups 2 and 3 and in the *P. violaceum* and *D. laterosorum* clade.

Fruiting body formation is often preceded by a period of slug migration, where slugs can either migrate freely or lay down a stalk while migrating. Slug migration occurs in all four ta-xon groups, but is most common among Group 4 species (Fig. 3, column 7). A small cluster of Group 4 species and a single non-Group 4 species, *D. polycephalum,* however, are the only ones to show free migration, suggesting that this character has evolved twice independently.

Size and shape of fruiting bodies. A primary determinant of fruiting body (sorocarp) size is the number of cells that can be collected into one aggregate. However, most of the sorocarp size and shape variation depends on the extent and manner of subsequent aggregate subdivision (Fig. 3, columns 9-14). These characteristics are controlled by so-called organizing centers or "tips", the first of which appears as a small protrusion on top of a newly formed aggregate. Additional tips can appear during streaming aggregation, breaking up streams into smaller aggregates. This gives rise to a gregarious sorocarp habit. Alternatively, multiple tips may appear on completed aggregates, giving rise to a clustered or coremiform (bunched) habit.

The rising cell masses (sorogens) that form the sorocarps can subdivide even further, forming secondary spore heads. This can occur either by new tips arising along the main so-rogen axis, yielding lateral branches, or by groups of cells detaching themselves from the rear of the sorogen. The latter abstricted masses can differentiate directly into spores to yield sessi-le sori (spore heads), as in *D. rosarium* (*16*), or form new tips giving rise to whorls of branches that are either irregular as in *D. tenue* (*17*) or evenly spaced as in the polysphondylids (18t).

Species in Groups 1-3 usually display a clustered or gregarious sorocarp habit, while Group 4 species mainly form solitary fruiting bodies (Fig. 3, column 9). Additionally, branched forms are much more common in Groups 1-3 than in Group 4. However, both lateral and whorled-type branching are found in most groups (Fig. 3, column 10). Not surprisingly, there is an inverse relationship between a tendency for aggregates and sorogens to subdivide and the size of stalk and sorus. Thus, the Group 4 species with their consolidated aggregates also have the largest sori and the thickest and longest stalks (Fig. 3, columns 11-13).

Other characteristics, such as the presence of support structures formed from stalk-like cells such as basal disks, triangular supporters or crampons, also appear to be markedly correlated with large fruiting body size, particularly in Groups 3 and 4 (Fig. 3, column 14). Group 4 especially appears to be the culmination of an evolutionary trend towards larger-sized units of stalk and spore-head. This trend was accompanied by increased cell-type specializa-tion resulting in the formation of robust stalk support structures.

Conclusions

We present the first molecular phylogeny of the social amoebas based on two independent markers. The use of two structurally and functionally unrelated genes, in this case SSU rRNA and α-tubulin, is critical to control for gene-specific artefacts to which all single gene trees are vulnerable (B. Elgie, P. Schaap and S. Baldauf, unpublished results).
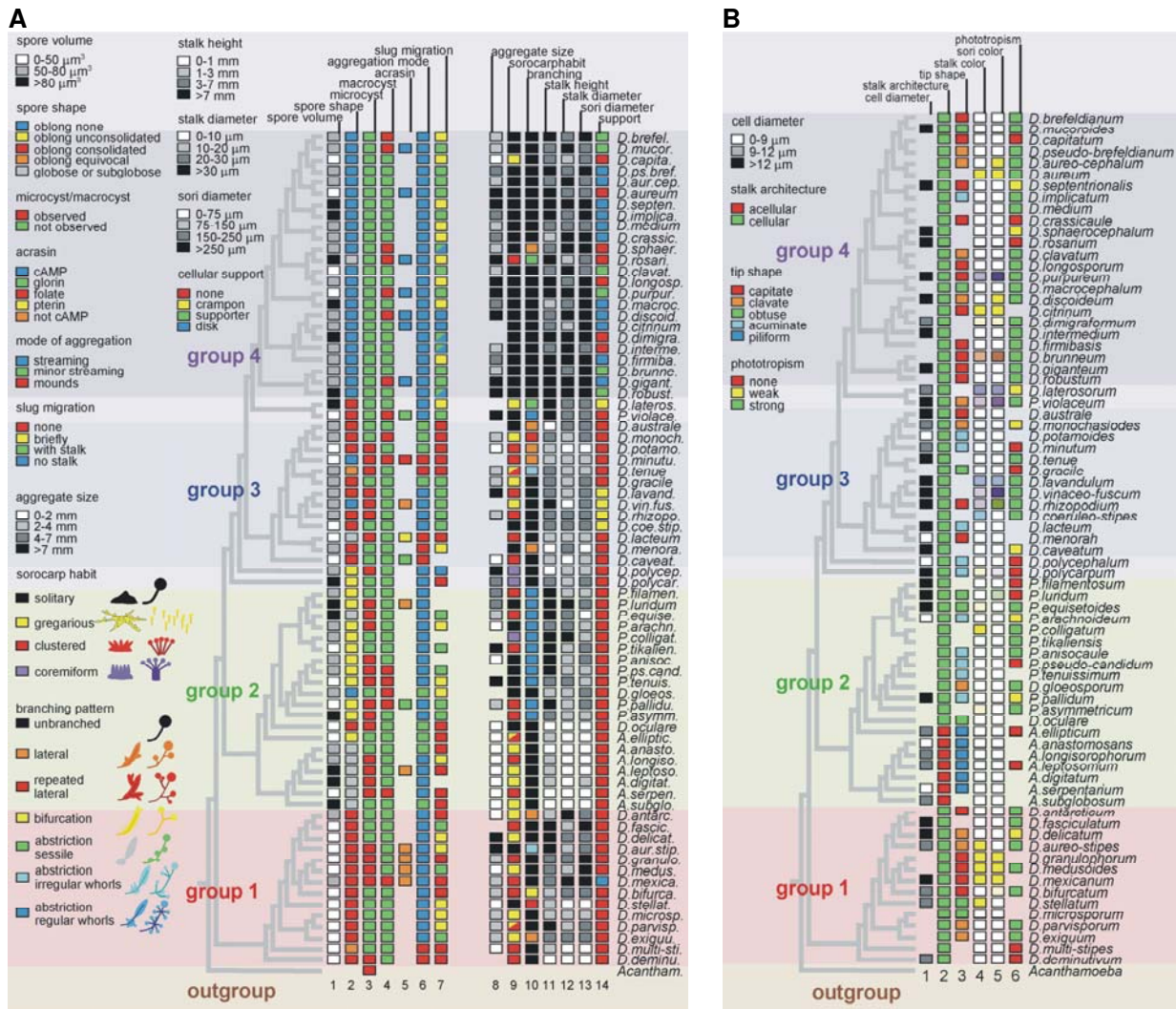
Figure 3. Trait mapping of dictyostelid characters (A) Consistently documented characters were retrieved from primary species descriptions (Table 1) and from *Dictyostelium* monographs (*2,24*). Character states were numerically coded and mapped to the dictyostelid SSU rRNA phylogeny (Fig. 1) using the MacClade 4 software package (*25*). For comprehensive presentation the most informative characters are combinatorially presented on a single tree with the numerical code converted into colour code for qualitative traits and into greyscale for quantitative traits. The code key for the character states is shown on the left side of the figure and in Table 2 (see main text for details). (B) An additional six characters were mapped onto the dictyostelid SSU rRNA phylogeny. Cell size, though inconsistently documented, shows no strong group-specific trend (column 1). A very restricted trait is the acellular stalk, which is found only in a subset of Group 2 species, the acytostelids (column 2). The tips of acellular stalks are thinly pointed (piliform) (column 3). Pointy (acuminate) or blunt (obtuse) tips also mark the cellular stalks of other group 2 species and of some group 3 species. Group 1 and Group 4 species usually have extended (capitate or clavate) stalk tips. Another character that is of importance for taxonomy is the color of the spores and stalk. This is represented here as an approximation of the observed color. Species with similarly coloured stalks and spore heads are often related, but no colour is specific for any of the four major groups (columns 4 and 5). *D. discoideum* slugs show phototaxis and thermotaxis, but these properties have rarely been investigated for other species. However, a related character is phototropism, the tendency of fruiting structures to veer towards the light (*1*). This trait appears to be common to all four groups, but not to all species within the groups (column 6).

In addition, congruent support from independent data is the strongest form of proof in evolutionary study (*19*). SSU rRNA was chosen for the primary phylogeny because it is a powerful and highly tractable phylogenetic marker, backed by the single most taxonomically broad molecular database available (*20*). A taxonomically broad sampling of α-tubulin sequences was then determined to test all major features of the SSU rRNA tree.

Thus, phylogenetic analyses of two independent molecular markers, SSU rRNA and α-tubulin, consistently subdivide nearly all dictyostelid species into four major groups with strong support from one or both molecules. Both trees also strongly support a Group 3 plus 4 supergroup, and both SSU rRNA (Fig. 1), and combined SSU rRNA plus weighted α-tubulin nucleotide sequences (*27*) place Group 1 as the earliest branching lineage in the tree. However, the

latter remains to be confirmed with additional data, as α-tubulin lacks adequate phylogenetic signal to resolve the deepest branches in the tree (Fig. 2) and combined analyses of only these two very disparate genes can only provide weak additional support (*27*). Although more limited sampling of EF1α data also confirms several of the major trends in the SSU rRNA and α-tubulin trees, interpretation of the EF1α data is complicated by multiple gene duplications within Dictyostelia (B. Elgie, P. Schaap and S. Baldauf, unpublished results).

None of the four major groups identified in the new molecular phylogeny correspond to traditional dictyostelid classification. The molecular tree is dominated by *Dictyostelium* species, which appear in all four groups. Most surprisingly, *Polysphondylium*s are found in two separate locations, within Group 2 and at the base of Group 4. This split of purple and pale polysphon-dylid species is supported by phylogenetic analyses both SSU rRNA (Fig. 1) and α-tubulin (Fig. 2), and by a cladistic analysis of morphological traits (*21*). While the *Acytostelium*s probably all reside in Group 2, this group also includes *Dictyostelium* and *Polysphondylium* species. Therefore, none of the four molecularly defined dictyostelid groups correspond to traditional genera, and none of the traditional genera, with the possible exception of *Acytostelium*, are even monophyletic. This indicates that fruiting body morphology is a very plastic trait in Dictyostelia and is apparently of little use as a taxonomic determinant. This is even more evident from the scattered distribution of similar branching morphologies over the four taxon groups (Fig. 3, columns 9-10). For instance, the rosary-type, coremiform and laterally branched morphologies appear respectively two, three and seven times independently across the tree.

The strongest evolutionary trend in dictyostelid fruiting body morphology appears to be related to size. Within each group the more derived species tend to have larger fruiting bodies, but this is most clearly shown when comparing entire groups. Whereas the species in Groups 1, 2 and 3 generally split up their aggregates into multiple sorogens, which then subdivide even further to yield branched fruiting bodies, the aggregates of Group 4 species usually give rise to a solitary fruiting body that is only rarely branched. As a result, the Group 4 species have more robust fruiting structures with much larger spore heads than the other groups. These large structures are typically supported at their base by basal discs or triangular supporters that are derived from a third cell-type, the anterior-like cells. In at least one species, *D. discoideum*, this cell-type diverges even further to produce two more structures, the upper- and lower cup that support the spore head. This is an interesting example of the correlation between the size of an organism and its cell-type diversity, which marks the evolution of many multicellular organisms (*22*).

To conclude, we have defined a radically new phylogeny for a major taxonomic group that includes an important model organism, and we have mapped a variety of morphological and behavioral characteristics onto the tree. The phylogeny suggests that Dictyostelia is a molecularly deep and complex group that is in need of major taxonomic revision. This new dictyostelid phylogeny also indicates that many widely studied characteristics of the group are highly plastic and therefore probably controlled by a small number of genes. This means that, using the new phylogeny as a guide, Dictyostelia is now uniquely well suited for unravelling the underlying mechanisms controlling these phenomena and thereby to add important infor-mation to our understanding of fundamental aspects of the evolution of eukaryotic cell-cell signalling and multicellularity.

Compilation of data used in the trait analsis represented in Figure 3.

Table 1. Consistently documented characters were retrieved from the original species diagnoses and from secondary publications, such as the *Dictyostelium* monographs by Raper and Hagiwara (1,15). The varieties (states) described for qualitative characters, such as the shapes of spores or the branching patterns of fruiting bodies were numerically coded. The alphabetical code key for each character and the numerical code key for each character state are listed in table 2. For quantitative characters (usually size) a frequency distribution of data for all species was prepared first, and the data range was subdivided into 3-4 intervals in such a manner that each interval contained about the same number of species. Each interval then represents a character state, which was again numerically coded as shown in table 2. Quantitative characters have usually been reported as a range of observed values. For trait mapping this range had to be reduced to a single parameter. For characters such as the size of aggregates, stalks and sori, the upper and intermediate value of the range were first analysed separately. However, this revealed virtually identical trends in character evolution (data not shown). We chose to show the analysis of the upper values here, because this is a better indication of the maximal number of cells that can be incorporated into a single structure (all species will form small structures when few cells are available, but only few will form large structures at high cell densities). For spore and cell sizes, intermediate values were used or average values, when reported. Spore sizes were usually reported as length (L) and width (w) of oblong spores and diameter (d) of globose spores. These values were further reduced to a single parameter by calculating the volume of oblong spores as a cylinder ($L\pi(\frac{1}{2}w)^2$) and that of globose spores as a sphere ($\frac{4}{3}\pi (\frac{1}{2}d)^3$).

Species	Character	Character states																		Citation
		A	B	C	D	E	F	G	H	I	J	K	L	M	N	O	P	Q	R	
D.brefeldianum		1	0	1	0	?	2	1	1	4	0	3	2	3	2	?	0	0	2	(15, 16)
D.mucoroides		1	0	1	0	0	2	2	1	4	0	2	3	2	2	2	0	2	2	(1, 15, 17)
D.capitatum		0	0	1	1	?	2	1	0	0	0	2	1	2	0	?	0	0	0	(15, 18)
D.pseudo-brefeldia.		1	0	1	1	?	2	2	2	4	0	3	2	3	3	?	0	1	2	(19)
D.aureocephalum		1	0	1	1	?	2	2	1	4	0	2	3	2	3	?	0	1	2	(20)
D.aureum		0	0	1	1	0	2	2	3	4	0	3	2	2	0	?	0	?	2	(1, 21, 22)
D.septentrionalis		2	0	1	1	?	2	1	3	4	0	3	3	3	3	2	0	0	1	(1, 15, 23)
D.implicatum		2	0	1	1	?	2	2	2	4	0	3	2	3	3	?	0	3	2	(15, 24)
D.medium		1	0	1	1	?	2	1	1	4	0	2	2	2	3	?	0	?	2	(25)
D.crassicaule		1	0	1	1	?	2	1	2	4	0	1	3	3	3	?	0	0	0	(15, 24)
D.sphaerocephalum		1	0	1	0	?	2	3	1	4	1	2	3	3	0	2	0	?	1	(1, 26, 27)
D.rosarium		2	5	1	0	0	2	1	3	2	4	3	1	2	0	2	0	?	0	(1, 28)
D.clavatum		0	0	1	1	?	2	2	1	4	0	2	3	2	2	?	0	1	2	(25)
D.longosporum		1	0	1	1	?	2	1	3	4	0	3	2	3	0	?	0	0	2	(29)
D.purpureum		0	0	1	0	0	2	2	3	4	0	3	3	3	2	2	0	0	2	(1, 15, 30)
D.macrocephalum		2	0	1	1	?	2	1	2	4	0	1	2	3	3	?	0	2	2	(15, 31)
D.discoideum		1	0	1	0	0	2	4	3	4	0	2	3	3	3	2	0	1	2	(1, 15, 32)
D.citrinum		1	0	1	1	0	2	4	?	4	0	2	1	3	3	?	0	0	?	(33)
D.dimigraformum		2	0	1	1	?	2	3	?	4	0	3	3	3	0	1	0	?	2	(1, 34)
D.intermedium		1	0	1	1	?	2	3	1	4	0	2	3	2	0	2	0	?	2	(1, 35)
D.firmibasis		1	0	1	1	?	2	1	2	4	0	3	3	3	3	?	0	0	2	(1, 15, 27)
D.brunneum		1	0	1	1	?	2	2	1	4	0	3	2	3	2	?	0	0	2	(1, 36)
D.giganteum		1	0	1	0	0	2	2	3	4	0	3	3	3	3	2	0	0	2	(1, 37-39)
D.robustum		2	0	1	1	?	2	3	3	4	0	3	3	3	4	?	0	0	2	(19)
D.laterosorum		2	2	1	1	?	2	1	?	0	4	3	2	2	1	1	0	?	1	(1, 34)
P.violaceum		0	2	1	0	3	2	2	3	4	6	3	2	2	0	2	0	1	2	(1, 15, 40)

D.australe	1	2	1	1	?	1	0	?	4	1	0	2	2	0	2	0	?	?	(41)
D.monochasioides	1	2	1	0	?	1	2	1	0	2	2	1	2	0	1	0	1	1	(1, 15, 42, 43)
D.potamoides	0	2	0	1	?	1	0	0	2	1	1	0	0	0	0	0	?	?	(44)
D.minutum	0	0	0	0	1	0	0	?	2	1	1	1	1	0	1	0	3	0	(1, 15, 45)
D.tenue	1	3	0	1	?	0	0	1	1	5	2	1	1	0	2	0	?	2	(1, 46)
D.gracile	1	2	1	1	?	1	2	1	0	0	2	1	2	0	?	0	2	0	(29)
D.lavandulum	1	2	0	1	?	2	2	3	2	0	2	1	2	1	2	0	?	2	(1, 15, 47)
D.vinaceo-fuscum	1	0	0	1	4	2	2	?	0	0	3	0	2	1	2	0	?	2	(1, 47, 48)
D.rhizopodium	1	2	0	1	?	2	2	1	2	0	2	2	2	1	2	0	0	2	(1, 15, 47)
D.coeruleo-stipes	0	2	1	1	?	2	2	?	4	0	2	2	2	1	?	0	?	2	(1, 47)
D.lacteum	0	4	0	1	2	0	0	?	2	0	1	1	1	0	2	0	3	?	(1, 49)
D.menorah	1	2	1	1	?	0	1	?	4	1	0	2	0	0	0	0	0	?	(50)
D.caveatum	0	2	1	1	3	0	?	0	2	0	1	0	1	0	2	0	?	1	(1, 51)
D.polycephalum	1	1	0	1	?	2	4	3	3	0	0	1	1	0	0	0	3	0	(1, 15, 52)
D.polycarpum	2	1	1	1	?	2	0	2	3	0	2	1	2	0	2	0	3	0	(1, 53)
P.filamentosum	1	1	1	1	?	2	?	2	2	6	3	1	1	0	2	0	?	0	(1, 53)
P.luridum	2	1	0	1	4	2	?	2	4	6	3	3	2	0	2	0	2	0	(54)
P.equisetoides	2	4	0	1	?	2	2	1	2	6	3	2	0	0	2	0	2	2	(55)
P.arachnoideum	1	1	0	1	?	2	1	0	4	6	2	2	1	0	0	0	3	1	(56)
P.colligatum	1	1	1	1	?	2	?	?	3	6	3	3	1	0	?	0	?	2	(57)
P.tikaliensis	0	1	1	1	?	2	2	3	2	6	3	1	2	0	?	0	?	2	(57)
P.anisocaule	1	1	0	1	?	2	?	0	4	6	3	1	2	0	?	0	3	2	(41)
P.pseudo-candidum	1	1	0	0	?	2	2	?	4	6	3	1	1	0	?	0	3	0	(1, 15, 43, 58)
P.tenuissimum	0	1	0	0	?	2	1	3	4	6	3	2	1	0	?	0	3	?	(1, 15, 58)
D.gloeosporum	1	0	1	0	?	1	1	?	4	0	1	1	2	0	?	0	1	2	(59)
P.pallidum	0	1	0	0	3	2	2	1	2	6	3	1	2	0	2	0	3	1	(1, 15, 21)
P.asymmetricum	2	1	0	1	?	2	2	?	2	6	2	1	1	0	?	0	?	2	(57)
D.oculare	0	2	0	1	?	1	0	0	4	0	0	0	0	0	?	0	?	?	(44)
A.ellipticum	0	1	1	1	?	1	0	0	1	0	1	0	0	0	1	1	4	0	(1, 34)
A.anastomosans	1	4	1	1	?	1	0	0	0	0	0	0	0	0	0	1	?	?	(44)
A.longisorophorum	1	4	0	1	?	2	1	0	2	0	1	0	0	0	1	1	?	?	(44)
A.leptosomum	2	4	0	1	4	2	0	0	0	0	1	0	0	0	1	1	4	0	(1, 48, 60)
A.digitatum	2	4	0	1	?	2	?	0	0	0	1	0	1	0	?	1	4	?	(61)
A.serpentarium	0	4	0	0	?	2	0	0	2	0	0	0	0	0	0	1	?	?	(44)
A.subglobosum	2	4	1	1	?	1	0	0	0	0	0	0	0	0	1	1	?	?	(1, 35, 61)
D.antarcticum	1	2	1	1	?	2	0	0	0	1	1	3	2	0	?	0	?	2	(41)
D.fasciculatum	0	2	1	1	?	2	2	?	2	0	3	1	3	0	2	0	?	2	(1, 53)
D.delicatum	0	2	1	1	?	2	1	3	0	0	3	2	2	0	2	0	1	1	(1, 15, 27)
D.aureo-stipes	0	2	0	1	4	2	1	3	4	5	3	1	2	0	1	0	1	2	(1, 15, 46)
D.granulophorum	0	2	0	1	4	2	0	1	2	0	2	2	3	0	?	0	0	?	(33)
D.medusoides	0	2	0	1	4	2	2	0	0	0	2	1	3	0	?	0	0	2	(33)
D.mexicanum	1	2	0	0	4	2	0	1	2	0	2	3	3	3	2	0	0	?	(1, 22)
D.bifurcatum	0	2	1	1	?	2	0	1	2	3	1	2	2	0	1	0	0	2	(1, 35)
D.stellatum	0	2	1	1	?	2	1	0	4	2	1	0	0	0	1	0	2	?	(44)
D.microsporum	0	2	1	1	?	2	1	1	0	0	1	1	1	0	?	0	2	0	(1, 15, 62)
D.parvisporum	0	2	1	1	?	2	1	1	1	0	3	1	2	0	?	0	1	2	(15, 63)
D.exiguum	0	2	1	1	?	2	2	1	0	1	2	2	2	0	?	0	1	2	(29)
D.multi-stipes	0	3	1	1	?	0	0	0	2	0	1	0	0	0	?	0	?	0	(1, 35)
D.deminutivum	0	2	0	1	?	0	0	?	2	0	0	0	0	0	1	0	?	0	(1, 64)

Table 2. This table lists the letter code for character names and the numerical code for character states as are used in Table 1. The colour code for character states as used in figure 4 is indicated in the last column.

Character name	Code	Character state	Code	Colour code
Spore volume	A	0-50 μm^3	0	white
		50-80 μm^3	1	grey
		>80 μm^3	2	black
		not measured or unknown	?	absent
Spore shape and granule position	B	oblong, no polar granules	0	blue
		oblong, unconsolidated polar granules	1	yellow
		oblong, consolidated polar granules	2	red
		oblong, granule position equivocal	3	orange
		globose or subglobose	4	grey
Microcyst	C	observed	0	red
		not observed	1	green
Macrocyst	D	observed	0	red
		not observed	1	green
Acrasin	E	cAMP	0	blue
		glorin	1	green
		folate	2	red
		pterin	3	yellow
		not cAMP	4	orange
Mode of aggregation	F	mounds	0	red
		minor streaming	1	green
		streaming	2	blue
Slug migration	G	none	0	red
		briefly	1	yellow
		with stalk being formed	2	green
		with and without stalk	3	green/blue
		without stalk formation	4	blue
Aggregate size	H	0-2 mm	0	white
		2-4 mm	1	light grey
		4-7 mm	2	dark grey
		>7 mm	3	black
Sorocarp habit	I	gregarious (loosely grouped)	0	yellow
		gregarious and clustered	1	yellow/red
		clustered (closely grouped)	2	red
		coremiform (bunched)	3	purple
		solitary	4	black
Branching pattern	J	unbranched	0	black
		lateral branches	1	orange
		repeated lateral	2	red
		bifurcation	3	yellow
		abstriction from posterior - sessile	4	green
		abstriction - irregular whorls	5	light blue
		abstriction - regular whorls	6	dark blue
Stalk height	K	0-1 mm	0	white
		1-3 mm	1	light grey
		3-7 mm	2	dark grey
		>7 mm	3	black

Stalk diameter	L	0-10 μm	0	white
		10-20 μm	1	light grey
		20-30 μm	2	dark grey
		>30 μm	3	black
Sori diameter	M	0-75 μm	0	white
		75-150 μm	1	light grey
		150-250 μm	2	dark grey
		> 250 μm	3	black
Cellular support	N	none	0	red
		crampon	1	yellow
		supporter	2	green
		disk	3	blue
Cell diameter	O	0-9 μm	0	white
		9-12 μm	1	grey
		>12 μm	2	black
Stalk shape	P	cellular	0	green
		acellular	1	red
Stalk tip shape	Q	capitate (head-shaped)	0	red
		clavate (club-shaped)	1	orange
		obtuse (blunt)	2	green
		acuminate (pointed)	3	light blue
		piliform (thread-shaped)	4	dark blue
Phototropism	R	none	0	red
		weak	1	yellow
		strong	2	green

I. References (Main Text)

1. S. M. Adl *et al.*, (2005) *J Eukaryot Microbiol* 52, 399
2. K. B. Raper, (1984) *The Dictyostelids* (Princeton University Press, Princeton, New Jersey)
3. J. F. Fahrni *et al.*, (2003) *Mol. Biol. Evol.* 20, 1881.
4. R. H. Kessin, (2001) *Dictyostelium:* Evolution, cell biology and the development of multicellularity (Cambridge University Press, Cambridge, UK.
5. L. Eichinger *et al.*, (2005) *Nature* 435, 43.
6. J. E. Strassmann, Y. Zhu, D. C. Queller, (2000) *Nature* 408, 965.
7. D. C. Queller, E. Ponte, S. Bozzaro, J. E. Strassmann, (2003) *Science* 299, 105.
8. E. Alvarez-Curto *et al.*, (2005) *Proc. Natl. Acad. Sci. USA* 102, 6385.
9. *D.mucoroides appears in three separate clades in Group 4. This is partly because the original holotype of Brefeld (26) was lost, and subsequent researchers made different diagnoses of more recent isolates. Hagiwara's D. mucoroides (TNS-C-114) is diagnosed by Raper as D. sphaerocephalum, while Raper's D. mucoroides (S28b) would be diagnosed as D. brefeldianum by Hagiwara.*
10. F. E. Anderson, D. L. Swofford, (2004) *Mol. Phylogenet. Evol.* 33, 440.
11. H. Brinkmann, M. Giezen, Y. Zhou, G. P. Raucourt, H. Philippe, (2005) *Syst. Biol.* 54, 743.
12. S. L. Baldauf, A. J. Roger, I. Wenk-Siefert, W. F. Doolittle, (2000) *Science* 290, 972.
13. E. Bapteste *et al.*, (2002) *Proc. Natl. Acad. Sci. USA* 99, 1414.
14. S. B. Hedges, S. Kumar, (2004) *Trends Genet.* 20, 242.
15. A.M. Aguinaldo *et al.*, (1997) *Nature* 387, 489.
16. K. B. Raper, J. C. Cavender, (1968) *J.Elisha Mitchell.Sci.Soc.* 84, 31.
17. J. C. Cavender, K. B. Raper, A. M. Norberg, (1979) *Amer.J.Bot.* 66, 207.
18. F. W. Spiegel, E. C. Cox, (1980) *Nature* 286, 806.
19. M. M. Miyamoto, W. M. Fitch, (1995) *Syst. Biol.* 44, 64.
20. J. Wuyts, G. Perriere, Y. V. de Peer, (2004) *Nucl. Acids Res.* 32, D101.
21. A.R. Swanson, F. W. Spiegel, J. C. Cavender, (2002) *Mycologia* 94, 968.
22. J. T. Bonner, (2004) *Evolution* 58, 1883.
23. S. I. Nikolaev *et al.*, (2005) *Protist* 156, 191.
24. H. Hagiwara, (1989) *The taxonomic study of Japanese Dictyostelid cellular slime molds.* (Nat.Science Museum, Tokyo) pp. 131.
25. W. P. Maddison, D. R. Maddison, (1989) *Folia Primatol (Basel)* 53, 190.
26. O. Brefeld, (1869) Abh. Senckenberg. Naturforsch. Ges. 7, 85.
27. Schaap, P., Winckler, T., Nelson, M., Alvarez-Curto, E., Elgie, B., Hagiwara, H., Cavender, J., Milano-Curto, A., Rozen, D. E., Dingermann, T.*, et al.* (2006). *Science* 314, 661-663.

II. References (Materials and Methods, Table 1)

1. K. B. Raper, *The Dictyostelids* (Princeton University Press, Princeton, New Jersey, 1984)
2. L. Medlin, H. J. Elwood, S. Stickel, M. L. Sogin, *Gene* 71, 491 (1988).
3. E. S. Steenkamp, J. Wright, S. L. Baldauf, *Mol. Biol. Evol.* in press (2005).
4. L. Nitschke, M. Kopf, M. C. Lamers, *Biotechniques* 14, 914 (1993).
5. T. A. Hall, *Nucl. Acids. Symp. Ser.* 41, 95 (1999).
6. J. D. Thompson, T. J. Gibson, F. Plewniak, F. Jeanmougin, D. G. Higgins, *Nucl. Acids Res.* 25, 4876 (1997).
7. D. L. Swofford, *PAUP*. Phylogenetic Analysis Using Parsimony (*and other methods). Version 4* (Sinauer Associates, Sunderland, Massachusetts, 1998).
8. S. L. Baldauf, A. J. Roger, I. Wenk-Siefert, W. F. Doolittle, *Science* 290, 972 (2000).
9. F. Ronquist, J. P. Huelsenbeck, *Bioinformatics* 19, 1572 (2003).
10. J. Felsenstein, G. A. Churchill, *Mol. Biol. Evol.* 13, 93 (1996).
11. S. Guindon, O. Gascuel, *Syst. Biol.* 52, 696 (2003).
12. S. Whelan, N. Goldman, *Mol. Biol. Evol.* 18, 691 (2001).
13. S. Gribaldo, H. Philippe, *Theor. Popul. Biol.* 61, 391 (2002).
14. M. Kimura, T. Ohta, *J. Mol. Evol.* 2, 87 (1972).
15. H. Hagiwara, in *The taxonomic study of Japanese Dictyostelid cellular slime molds.* (Nat.Science Museum, Tokyo, 1989).
16. H. Hagiwara, *Bull. Natn. Sc. Mus.* 10, 27 (1984).
17. O. Brefeld, *Abhandlungen der Senckenbergischen Naturforschenden Gesellschaft* 7, 85 (1869).
18. H. Hagiwara, *Bull. Natn. Sc. Mus.* 9, 45 (1983).
19. H. Hagiwara, *Bull. Natn. Sci. Mus.* 22, 47 (1996).
20. H. Hagiwara, *Bull. Natn. Sci. Mus.* 17, 103 (1991).
21. E. W. Olive, *Proc. Amer. Acad. Arts Sci.* 37, 333 (1901).
22. J. C. Cavender, A. C. Worley, K. B. Raper, *Amer. J. Bot.* 68, 373 (1981).
23. J. C. Cavender, *Can. J. Bot.* 57, 1326 (1978).
24. H. Hagiwara, *Bull. Natn. Sci. Mus. Tokyo* 10, 63 (1984).
25. H. Hagiwara, *Bull. Natn. Sci. Mus.* 18, 1 (1992).
26. C. A. J. A. Oudemans, *Aanwinsten voor de Flora Mycologia van Nederland* 9-10, 39 (1885).
27. H. Hagiwara, *Bull. Natn. Sci. Mus.* 14, 351 (1971).
28. K. B. Raper, J. C. Cavender, *J. Elisha Mitchell. Sci .Soc.* 84, 31 (1968).
29. H. Hagiwara, *Bull. Natn. Sci. Mus.* 9, 149 (1983).
30. E. G. Olive, *Proc. Boston Soc. Nat. His.* 30, 451 (1902).
31. H. Hagiwara, Z.-Y. Yeh, C.-Y. Chien, *Bull. Natn. Sci. Mus. Tokyo* 11, 103 (1985).
32. K. B. Raper, *J. Agric. Res.* 50, 135 (1935).
33. E. M. Vadell, M. T. Holmes, J. C. Cavender, *Mycologia* 87, 551 (1995).
34. J. C. Cavender, *J. Gen. Microbiol.* 62, 113 (1970).

35. J. C. Cavender, *Amer. J. Bot.* 63, 60 (1976).
36. K. Kawabe, *Trans. Mycol. Soc. Japan* 23, 91 (1982).
37. B. N. Singh, *J. Gen. Microbiol.* 1, 11 (1947).
38. H. Hagiwara, *Bull. Natn. Sci. Mus.* 18, 101 (1992).
39. H. Hagiwara, *Bull. Natn. Sci. Mus.* 24, 81 (1998).
40. O. Brefeld, *Unters. Gesammtgeb. Mykol.* 6, 1 (1884).
41. J. C. Cavender, S. L. Stephenson, J. C. Landolt, E. M. Vadell, *New Zealand J. Bot.* 40, 235 (2002).
42. H. Hagiwara, *Bull. Natn. Sci. Mus.* 16, 493 (1973).
43. S. Kawakami, H. Hagiwara, *Mycoscience* 40, 357 (1999).
44. J. C. Cavender, E. Vadell, J. C. Landolt, S. L. Stephenson, *Mycologia* 97, 493 (2005).
45. K. B. Raper, *Mycologia* 33, 633 (1941).
46. J. C. Cavender, K. B. Raper, A. M. Norberg, *Amer. J. Bot.* 66, 207 (1979).
47. K. B. Raper, D. I. Fennell, *Amer. J. Bot.* 54, 515 (1967).
48. J. T. Bonner, *Amer. Nat.* 119, 530 (1982).
49. M. P. Van Tieghem, *Bull. de la Soc. Botan. de France* 27, 317 (1880).
50. J. Cavender, (unpublished results).
51. D. R. Waddell, *Nature* 298, 464 (1982).
52. K. B. Raper, *J. Gen. Microbiol.* 14, 716 (1956).
53. F. Traub, H. R. Hohl, J. C. Cavender, *Amer.J.Bot.* 68, 162 (1981).
54. G. Kauffman, J. Cavender, H. R. Hohl, *Botanica Helvetica* 98, 123 (1988).
55. J. C. Cavender, 8 (unpublished results).
56. E. M. Vadell, J. C. Cavender, (in prep.).
57. E. M. Vadell, J. C. Cavender, *Mycologia* 90, 715 (1998).
58. H. Hagiwara, *Bull. Natn. Sci. Mus.* 5, 67 (1979).
59. H. Hagiwara, *Bull. Natn. Sci. Mus.* 29, 127 (2003).
60. K. B. Raper, M. S. Quinlan, *J. Gen. Microbiol.* 18, 16 (1958).
61. J. C. Cavender, E. M. Vadell, *Mycologia* 92, 992 (2000).
62. H. Hagiwara, *Bull. Natn. Sci. Mus.* 4, 27 (1978).
63. H. Hagiwara, *Bull. Natn. Sci. Mus.* 12, 99 (1986).
64. J. S. Anderson, D. I. Fennell, K. B. Raper, *Mycologia* 60, 49 (1968).